DECISION ANALYSIS
Vol. 9, No. 4, December 2012, pp. 329–347
ISSN 1545-8490 (print) | ISSN 1545-8504 (online)

http://dx.doi.org/10.1287/deca.1120.0252

A Simulation-Based Approach to Decision Making with Partial Information

Luis V. Montiel, J. Eric Bickel
Graduate Program in Operations Research and Industrial Engineering, University of Texas at Austin, Austin, Texas 78712 {lvmontiel@utexas.edu, ebickel@mail.utexas.edu}

The construction of a probabilistic model is a key step in most decision and risk analyses. Typically this is done by defining a single joint distribution in terms of marginal and conditional distributions. The difficulty of this approach is that often the joint distribution is underspecified. For example, we may lack knowledge of the marginal distributions or the underlying dependence structure. In this paper, we suggest an approach to analyzing decisions with partial information. Specifically, we propose a simulation procedure to create a collection of joint distributions that match the known information. This collection of distributions can then be used to analyze the decision problem. We demonstrate our method by applying it to the Eagle Airlines case study used in previous studies.

Key words: decision analysis; dependence; simulation; sensitivity to dependence; copulas; Eagle Airlines
History: Received on April 5, 2012. Accepted on August 28, 2012, after 2 revisions. Published online in *Articles in Advance* October 26, 2012.

1. Introduction

In many decision problems, we lack complete information regarding the underlying joint probability distribution. For example, marginal distributions and/or probabilistic dependencies may not be completely specified. Differing methodological areas within the management sciences view this lack of specificity in differing ways. To some, the lack of information stems from a belief that the underlying probability distribution is "unknown." Others regard the incomplete information as simply an acknowledgment that it has yet to be assessed. We do not distinguish between these perspectives in this paper. Instead, we present a methodology that is useful in either case. For those that believe the underlying distributions are unknown, our procedure will allow them to model this uncertainty explicitly. For those that see this as an issue of assessment, the methods discussed herein will help to ensure that the assessed distributions are consistent with the available information and quantify the benefit of further elicitations.

Although the lack of information could stem from an under specification of marginal distributions, we are primarily motivated by underspecification of the probabilistic dependence structure. Probabilistic dependencies are inherent to many decision environments, including medicine (Chessa et al. 1999), nuclear power (Cooke and Waij 1986), and oil exploration (Bickel and Smith 2006, Bickel et al. 2008). Failure to capture these relationships can have important and sometimes tragic consequences (Apostolakis and Kaplan 1981, Smith et al. 1992). For example, the Space Shuttle Challenger accident was apparently caused, in part, by engineers' failure to understand the dependency between ambient temperature and o-ring resiliency (Presidential Commission on the Space Shuttle Challenger Accident 1986).

Probabilistic dependence is often ignored because it complicates probability assessments (Lowell 1994, Korsan 1990). Winkler (1982) identified the assessment and modeling of probabilistic dependence as one of the most important research topics facing decision analysts. He suggested the development of sensitivity analyses that would identify key dependencies and decision-making methods that use less than full probabilistic information. Miller (1990, p. 443) argued, "We need a way to assess and process dependent probabilities efficiently. If we can find generally applicable methods for doing so, we could make significant advances in our ability to analyze and model

complex decision problems." These critical challenges have gone largely unanswered.

In this paper, we present a new methodology for modeling decisions given partial probabilistic information. In particular, we create the set of all possible discrete distributions that are consistent with the information that we do have. We then (uniformly) sample from this set using the joint distribution simulation (JDSIM) procedure (Montiel 2012, Montiel and Bickel 2012), which is based on the hit-and-run sampler (Smith 1984). Our procedure is perhaps best thought of as a sensitivity analysis, because we do not claim that all distributions in our set are equally likely. Indeed, specifying the probability distribution over the set of all probability distributions presents its own difficulties.

Other approaches to the problem discussed here fall into three primary categories: (i) approximation methods that specify a single joint probability distribution given partial information, (ii) sensitivity analysis procedures that partially explore the space of feasible joint distributions, and (iii) "robust" decision-making methods that attempt to ensure some minimum level of performance.

The most prominent example in the first category is the maximum entropy method (maxent) pioneered by Jaynes (1957, 1968), in which a single distribution (the one that is most uncertain, or has the highest entropy) is selected from the set of all possible distributions that are consistent with the given information. This approach was further developed by Ireland and Kullback (1968), who were the first to approximate a discrete joint distribution given information on the lower-order component distributions. Lowell (1994) also used maxent to specify a joint distribution given lower-order assessments (e.g., pairwise conditional assessments). More recently, Abbas (2006) and Bickel and Smith (2006) explored the use of maxent to facilitate the modeling of dependence.

A closely related approach is the specification of a copula (Sklar 1959), which encodes the dependence between marginal distributions. For example, Jouini and Clemen (1996), Frees et al. (1996), and Clemen and Reilly (1999) all used copulas to construct joint distributions based on lower-order assessments. In the copula-based approach, the continuous joint distribution is often discretized to facilitate modeling within a discrete decision-tree framework. In this paper, we compare our proposed methodology to the normal-copula (NC) approach, illustrated by Clemen and Reilly (1999) (hereafter, CR).

In the second category, sensitivity procedures have been developed to explore portions of the set of possible joint distributions. For example, Lowell (1994) developed a sensitivity analysis procedure to identify important pairwise conditional probability assessments. As discussed above, CR proposed the use of a normal copula, characterized by pairwise correlation coefficients. They then perturbed the correlation matrix to explore a set of possible joint distributions. This set is restricted to joint distributions that can be modeled with a normal copula. Reilly (2000) developed a sensitivity approach that uses synthetic variables based on a pairwise correlation coefficient matrix.

Finally, in the third category, robust procedures such as maximin or robust optimization (Ben-Tal et al. 2009) evaluate decisions based on their worst possible outcomes. We do not directly address these methods. We note, however, that identifying the worst possible joint distribution is often difficult. Our procedure could be used in a robust setting to "stress test" decisions.

This paper is organized as follows. Section 2 describes a new procedure to generate joint probability distributions when only partial information is available. Section 3 introduces an illustrative example that we use to demonstrate our approach. Section 4 applies our new procedure to this example. Section 5 concludes and discusses future research directions.

2. Proposed Approach

Montiel (2012) developed the JDSIM procedure, and Montiel and Bickel (2012) showed how JDSIM can be used to generate random collections of joint distributions. In this paper, we demonstrate how to use JDSIM to model decision problems with incomplete information and compare our procedure to the use of copulas. In this section, we summarize JDSIM and refer the interested reader to Montiel and Bickel (2012) for additional details.

JDSIM samples from the set of all possible discrete joint distributions that are consistent with the given

information, provided that this information can be described by a set of linear constraints. In this way, JDSIM provides not one, but a collection of discrete joint distributions under which the decision can be evaluated. The procedure begins with the specification of linear constraints on the joint distribution (e.g., specification of marginal probabilities or pairwise correlations) and the creation of a convex polytope $\mathbb{T}$, the "truth set," that matches the given information. By "truth" we mean that any distribution within this set is consistent with the assessments and therefore could be the "true" joint distribution.

We illustrate the characterization of $\mathbb{T}$ using a simple example with two binary random variables, V_1 and V_2. This distribution has four joint events (Figure 1(a)), whose probabilities must be positive and sum to one (Figure 1(b)). The truth set can be expressed as a hyperplane in four dimensions or as a full-dimensional polytope in three dimensions (Figure 1(c)). We can constrain $\mathbb{T}$ to match marginal assessments such as $P(V_2 = \text{Up}) = P_1 + P_3 = 0.6$, as shown in Figure 1(d). When constraints are consistent, nonredundant, and nondegenerate, each constraint reduces the dimension of $\mathbb{T}$ by one. Then, adding a second marginal constraint will reduce $\mathbb{T}$ to a one-dimensional line, and adding a correlation constraint will reduce $\mathbb{T}$ to a single point. Note that the addition of inconsistent constraints (assessments) produces an infeasible set. Hence, for the remainder of this paper, we assume that all assessed information is consistent such that $\mathbb{T}$ is not empty.

Formally, we can define the truth set as $\mathbb{T} = \{\mathbf{p} \mid \mathbf{Ap} = \mathbf{b}, \mathbf{p} \geq 0\}$, where $\mathbf{A} \in \mathbb{R}^{m,n}$ is a matrix of m rows and n columns, $\mathbf{b} \in \mathbb{R}^m$ is a column vector of assessed information, and $\mathbf{p} \geq 0$ is a vector that represents the joint probability distribution. The linear system, $\mathbf{Ap} = \mathbf{b}$, defining the truth set from Figure 1 is

$$\begin{bmatrix} 1 & 1 & 1 & 1 \\ 1 & 0 & 1 & 0 \end{bmatrix} \begin{bmatrix} P_1 \\ P_2 \\ P_3 \\ P_4 \end{bmatrix} = \begin{bmatrix} 1 \\ 0.6 \end{bmatrix}. \tag{1}$$

2.1. Truth Set Definition

We now introduce the notation that we use to define $\mathbb{T}$. We organize this notation into three groups: *indices and sets*, *data*, and *explored variables*. *Indices and sets* describe the notation used to create the structural constraints. *Data* represents the input information. *Explored variables* are the probabilities of the joint events that define the discrete joint distributions.

2.1.1. Notation.

Indices and Sets:

- $\mathbb{V}$: Ordered set of random variables indexed by $i = 1, \ldots, v$.
- $\mathbb{O}^i$: Ordered set of possible outcomes for random variable i indexed by $r_i = 1, 2, \ldots, |\mathbb{O}^i|$.
- $\omega^i_{r_i} \in \mathbb{O}^i$: Realization for random variable i having outcome r_i.
- $\mathbb{U}$: Ordered set of all joint outcomes, $\mathbb{U} = \mathbb{O}^1 \times \mathbb{O}^2 \times \cdots \times \mathbb{O}^v$.
- $\omega_k \in \mathbb{U}$: Joint realization $\omega_k = (\omega^1_{r_1}, \omega^2_{r_2}, \ldots, \omega^v_{r_v})$ indexed by $k = 1, 2, \ldots, \prod_{i=1}^{v} |\mathbb{O}^i|$.
- $\mathbb{U}_{\omega^i_{r_i}} \subset \mathbb{U}$: Proper subset $\mathbb{U}_{\omega^i_{r_i}} = (\omega_k \mid \omega_k \in \mathbb{U}, \omega^i_{r_i} \in \omega_k)$.

Data:

- $q_{\omega^i_{r_i}}$: Probability that random variable i obtains the value $\omega^i_{r_i}$.
- $\rho_{i,j}$: Rank correlation between random variables i and j.

Explored Variables:

- $\mathbf{p}$: Vector of joint probabilities to be explored.
- $p_{\omega_k} \in \mathbf{p}$: Probability of the discrete joint outcome ω_k.

2.1.2. Illustration of the Notation. To illustrate the notation, we use the example in Figure 1.[1] The set of random variables $\mathbb{V} = (V_1, V_2)$ is indexed as $i = 1, 2$. The set of possible outcomes (i.e., branches on the decision tree) for V_1 and V_2 are $\mathbb{O}^1 = (\text{High, Low})$ and $\mathbb{O}^2 = (\text{Up, Down})$, respectively. These sets are indexed as $r_1 = 1, 2$ for High or Low and $r_2 = 1, 2$ for Up or Down, respectively. The notation $\omega^i_{r_i}$ refers to particular realizations (i.e., to particular branches). For example, $\omega^1_{r_1} = \text{High}$, $\omega^1_{r_2} = \text{Low}$, $\omega^2_{r_1} = \text{Up}$, and $\omega^2_{r_2} = \text{Down}$. In this example, the set of all joint outcomes is defined as $\mathbb{U} = (\omega_1, \omega_2, \omega_3, \omega_4)$, where $\omega_1 = (\omega^1_{r_1}, \omega^2_{r_1})$, $\omega_2 = (\omega^1_{r_1}, \omega^2_{r_2})$, $\omega_3 = (\omega^1_{r_2}, \omega^2_{r_1})$, and $\omega_4 = (\omega^1_{r_2}, \omega^2_{r_2})$. The proper subset $\mathbb{U}_{\omega^2_{r_1}} = (\omega_1, \omega_3)$ includes the elements of

[1] See the online supplement for a spreadsheet illustrating our notation and constraints, available at http://dx.doi.org/10.1287/deca.1120.0252.

Figure 1 Example Characterization of the Truth Set $\mathbb{T}$

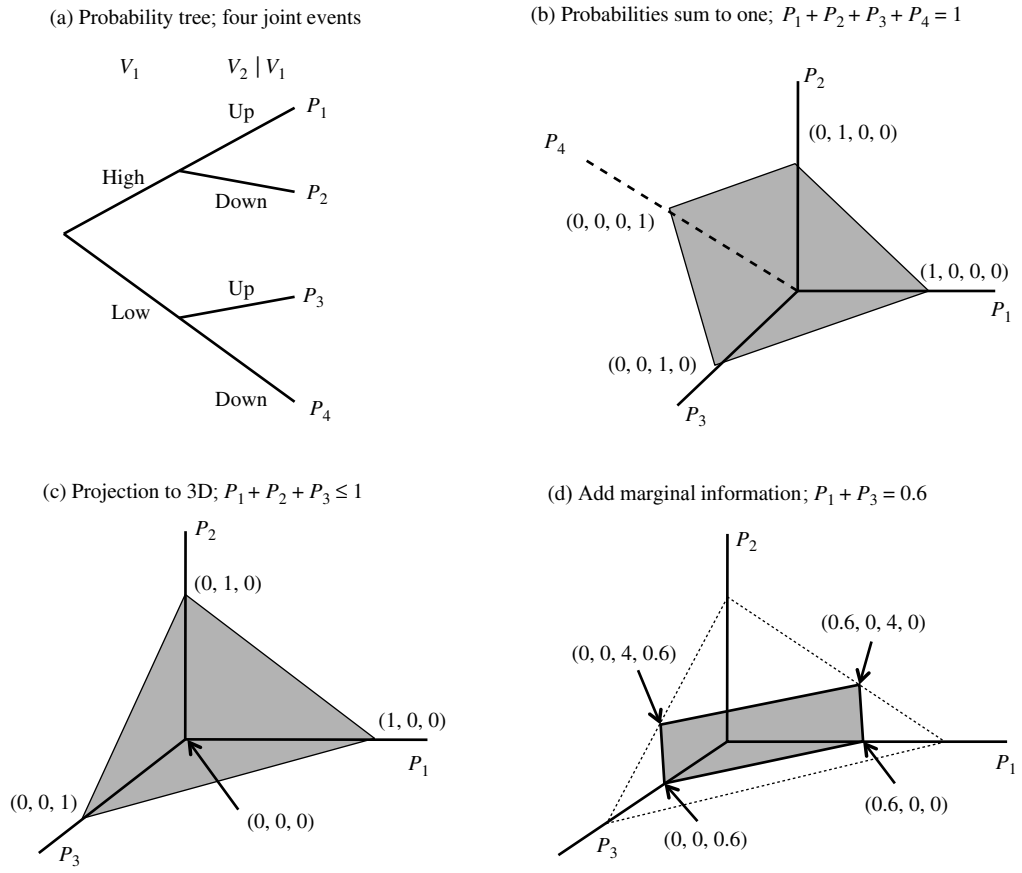

$\mathbb{U}$ for which realization $\omega^2_{r_1}$ has obtained (i.e., the first and third branches in Figure 1).

We require the joint probabilities to sum to one, which implies that $p_{\omega_1} + p_{\omega_2} + p_{\omega_3} + p_{\omega_4} = 1$. Likewise, the assessed probability $q_{\omega^2_{r_1}} \equiv P(V_2 = \text{Up}) = P(V_1 = \text{High}, V_2 = \text{Up}) + P(V_1 = \text{Low}, V_2 = \text{Up}) = p_{\omega_1} + p_{\omega_3} = 0.6$. The rank correlation $\rho_{1,2}$ between V_1 and V_2 was not used in Figure 1. Finally, the vector $\mathbf{p} = (p_{\omega_1}, p_{\omega_2}, p_{\omega_3}, p_{\omega_4}) \equiv (P_1, P_2, P_3, P_4)$ represents a feasible discrete joint probability distribution, which we will explore with our simulation procedure.

We now describe general forms of linear constraints that we consider in this paper.

2.1.3. Constraints for Necessary and Sufficient Conditions. First, we require $\mathbf{p} = (p_{\omega_1}, p_{\omega_2}, \ldots, p_{\omega_{|\mathbb{U}|}})$ to be a probability mass function (pmf). Equations (2a) and (2b) accomplish this by requiring the elements of $\mathbf{p}$ to sum to one and be nonnegative, respectively. In our matrix notation, the first row of $\mathbf{A}$ is a vector of ones, and the first element of $\mathbf{b}$ is a one, as in Equation (1). If no additional constraints are included, then $\mathbb{T}$ is the unit simplex, which is compact and convex. Therefore, the addition of other linear constraints will maintain the convexity of $\mathbb{T}$:

$$\sum_{\omega_k \in \mathbb{U}} p_{\omega_k} = 1, \tag{2a}$$

$$p_{\omega_k} \ge 0, \quad \forall\, \omega_k \in \mathbb{U}. \tag{2b}$$

2.1.4. Constraints for Marginal Distributions. Equation (3) constrains $\mathbb{T}$ to match the marginal assessments ($q_{\omega^i_{r_i}}$). This equation can be extended to cover pairwise, three-way, or higher-order joint probability information as long as the assessed beliefs are consistent. In this case, $\mathbf{A}$ includes a row of zeroes and ones, the arrangement of which depends upon

the random variable in question (see Equation (1)), and **b** adds one parameter $q_{\omega^i_{r_i}}$ for each constraint:

$$\sum_{\omega_k \in \mathbb{U}_{\omega^i_{r_i}}} p_{\omega_k} = q_{\omega^i_{r_i}} \quad \forall\, i \in \mathbb{V},\ \omega^i_{r_i} \in \mathbb{O}^i. \tag{3}$$

2.1.5. Constraints for Rank Correlations. Equation (4a) matches any rank correlation information (see Appendix A) that we might have, where we have used the definition of rank correlation provided by Nelsen (1991) and MacKenzie (1994). The $\gamma^{(i,j)}_{\omega_k}$ are coefficients calculated using Equations (4b), (4c), and (4d). Thus, Equation (4a) is linear in the joint probabilities. We now briefly discuss the other components of Equation (4a). Below, we show how to use Equation (4a) within the context of our example.

Equation (4c) corresponds to the *H-volume* defined by Nelsen (2005), and $\mathbf{B}_{\omega_k} = [I_{\omega_k}(V_i) \times I_{\omega_k}(V_j)]$ is the rectangular area defined by interval (4d).

$$\sum_{\omega_k \in \mathbb{U}} \gamma^{(i,j)}_{\omega_k} p_{\omega_k} = \frac{\rho_{i,j}+3}{3} \quad \forall\, i, j \in \mathbb{V}, \tag{4a}$$

$$\gamma^{(i,j)}_{\omega_k} = \frac{\mathbf{V}_{(xy)^2}[\mathbf{B}_{\omega_k}]}{q_{\omega^+_k(V_i)} \cdot q_{\omega^+_k(V_j)}} \quad \forall\, \omega_k \in \mathbb{U} \text{ and } i, j \in \mathbb{V}, \tag{4b}$$

$$\mathbf{V}_{(xy)^2}[\mathbf{B}_{\omega_k}] = (p^{i+}_k \cdot p^{j+}_k)^2 - (p^{i+}_k \cdot p^{j-}_k)^2 - (p^{i-}_k \cdot p^{j+}_k)^2 + (p^{i-}_k \cdot p^{j-}_k)^2, \tag{4c}$$

$$I_{\omega_k}(V_i) \equiv [p^{i+}_k, p^{i-}_k] \quad \text{and} \quad I_{\omega_k}(V_j) \equiv [p^{j+}_k, p^{j-}_k]. \tag{4d}$$

The cumulative probabilities $p^{i+}_k = P(V_i \le \omega^+_k(V_i))$ and $p^{i-}_k = P(V_i \le \omega^-_k(V_i))$ are defined such that $\omega^+_k(V_i)$ is the marginal outcome $\omega^i_{r_i}$ of random variable i at the joint realization ω_k, and $\omega^-_k(V_i)$ is the marginal outcome $\omega^i_{r_i-1}$ of the random variable i given the joint realization ω_k. Hence, $\omega^i_{r_i-1}$ is the marginal outcome immediately smaller than $\omega^i_{r_i}$ in the marginal distribution of the random variable i. Finally, $q_{\omega^+_k(V_i)} = P(V_i = \omega^+_k(V_i))$ is the marginal probability of variable V_i, having the outcome $\omega^i_{r_i}$ at the joint realization ω_k.

Equation (4a) requires that the marginal probabilities of V_i and V_j are known. Returning to our previous example in Figure 1, if we assume $q_{\omega^1_{r_1}} = 0.7$ and $q_{\omega^2_{r_1}} = 0.6$, then the truth set is reduced to a line with endpoints $(0.3, 0.4, 0.3, 0)$ and $(0.6, 0.1, 0, 0.3)$. The coefficients in Equation (4a) are

$$\gamma^{(1,2)}_{\omega_1} = \frac{(1\cdot 1)^2 - (1\cdot 0.4)^2 - (0.3\cdot 1)^2 + (0.3\cdot 0.4)^2}{0.7\cdot 0.6} = 1.82,$$

$$\gamma^{(1,2)}_{\omega_2} = \frac{(1\cdot 0.4)^2 - (1\cdot 0)^2 - (0.3\cdot 0.4)^2 + (0.3\cdot 0)^2}{0.7\cdot 0.4} = 0.52,$$

$$\gamma^{(1,2)}_{\omega_3} = \frac{(0.3\cdot 1)^2 - (0.3\cdot 0.4)^2 - (0\cdot 1)^2 + (0\cdot 0.4)^2}{0.3\cdot 0.6} = 0.42,$$

$$\gamma^{(1,2)}_{\omega_4} = \frac{(0.3\cdot 0.4)^2 - (0.3\cdot 0)^2 - (0\cdot 0.4)^2 + (0\cdot 0)^2}{0.3\cdot 0.4} = 0.12.$$

Hence, the rank correlation constraint is given by

$$1.82\cdot p_{\omega_1} + 0.52\cdot p_{\omega_2} + 0.42\cdot p_{\omega_3} + 0.12\cdot p_{\omega_4} = \frac{\rho_{i,j}+3}{3}. \tag{5}$$

Within the truth set, feasible rank correlations range from 0.54 at $(0.6, 0.1, 0, 0.3)$ to -0.36 at $(0.3, 0.4, 0.3, 0)$. Specifying a particular correlation within this range would reduce the truth set to a single point, uniquely specifying a joint distribution **p**.

2.2. Sampling $\mathbb{T}$

After characterizing $\mathbb{T}$, we uniformly sample **p** from the truth set using JDSIM. Our algorithm adapts the hit-and-run sampler (Smith 1984), which is the fastest known algorithm to uniformly sample the interior of an arbitrary polytope. The goal of this procedure is to create a discrete representation of $\mathbb{T}$ that replicates the dispersion of the distributions within the set. Figure 2 provides a graphical representation of the algorithm in two dimensions. Our procedure was explained in detail in Montiel and Bickel (2012), but we briefly summarize it here for convenience. The interested reader should see Montiel and Bickel (2012) for technical details, including convergence properties and guidance regarding the required number of samples.

The sampler is initialized (Step 1) by generating an arbitrary point $x_i \in \mathbb{T}$ and setting the counter $i = 0$. Step 2 generates a set of directions $D \subseteq \mathbb{R}^n$ using an uncorrelated multivariate standard-normal distribution and standardizing the directions. Step 3 selects a uniformly distributed direction $d_i \in D$. Step 4 finds the line $L = \mathbb{T} \cap \{x \mid x = x_i + \lambda d_i,\ \lambda \text{ a real scalar}\}$ generated by extending the direction d_i in both directions until the boundary of $\mathbb{T}$ is reached. Step 5 selects a random point $x_{i+1} \in L$ uniformly distributed over the line. Finally, Step 6 evaluates the counter and stops if $i = N$ (where N is the desired number of samples); otherwise the counter is incremented by one and the sampler returns to Step 2.

It is important to bear in mind that each sampled point is a complete joint pmf. We calculate the

Figure 2 Illustration of the Hit-and-Run Sampler in Two Dimensions

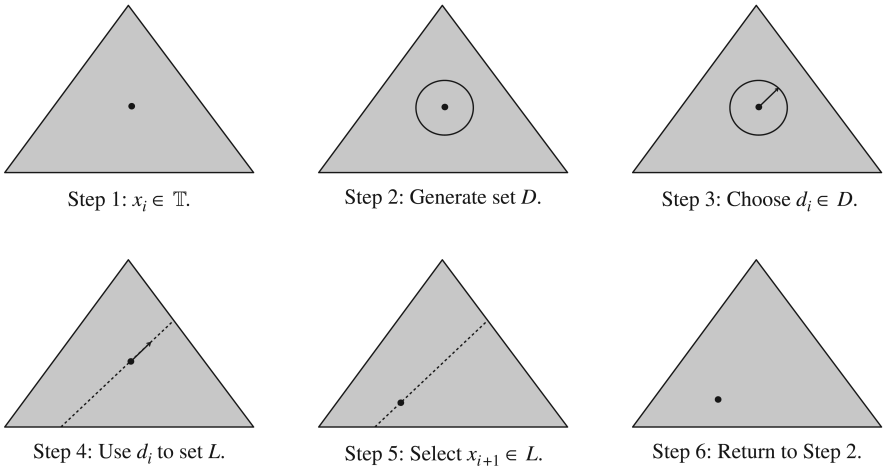

element-wise average of all sampled joint distributions and refer to this as the average of sampled observations (ASO). Because the ASO is a convex combination of points in $\mathbb{T}$, and $\mathbb{T}$ is convex, the ASO is a feasible joint distribution in $\mathbb{T}$.

3. Illustrative Example

We now describe the illustrative example that we use to demonstrate our procedure. The Eagle Airlines example was introduced by Clemen (1996) and later extended by Clemen and Reilly (1999) and Reilly (2000). See Figure 3. We describe the example with an excerpt from Reilly (2000, p. 559):

> Dick Carothers, the owner of Eagle Airlines, is deciding whether to invest . . . \$52,500 in a money market or to expand his fleet with the purchase of [an airplane; we will refer to this as the "Expand" alternative]. His decision criterion is whether the new plane will generate more profit than a money market alternative. The influence diagram in [Figure 3] illustrates the relevant variables. . . .
>
> The profit function is given by: *Profit* = *Total Revenue* − *Total Cost*, where
>
> *Total Revenue*
>
> = *Charter Ratio* ∗ *Hours Flown* ∗ *Charter Price*
>
> + (1 − *Charter Ratio*) ∗ *Hours Flown* ∗ *Capacity*
>
> ∗ *Number of Seats* ∗ *Price Level*,
>
> *Total Cost*
>
> = *Hours Flown* ∗ *Operating Cost* + *Insurance*
>
> + *Purchase Price* ∗ *Percentage Financed* ∗ *Interest Rate*,
>
> where *Charter Price* is 3.25 ∗ *Price Level* and the *Number of Seats* is five. Computing the profit using the base values [described below], Carothers's annual profit is \$9,975, which is \$5,775 more than the minimum of \$4,200 (based on the opportunity cost of capital). The deterministic model indicates that Carothers should expand his fleet now. Some of the inputs, however, are highly variable, and these could possibly lower the profit below the \$4,200 benchmark.

Based on sensitivity analysis, Reilly (2000) showed that four variables most affect the decision: *Price Level* (*PL*), *Hours Flown* (*H*), *Capacity* (*C*), and *Operating Cost per Hour* (*O*). CR provided the 0.10 (Low), 0.50 (Base), and 0.90 (High) fractiles for each uncertainty and the Spearman rank correlations between each pair of uncertainties, which we repeat in Table 1.

The noncritical uncertainties are fixed at their base values, which are *Charter Ratio* = 50%, *Percentage Financed* = 40%, *Interest Rate* = 11.5%, *Insurance* = \$20,000, *Purchase Price* = \$87,500, *Number of Seats* = 5, and *Charter Price* = 3.25 ∗ *Price Level*.

To apply their NC procedure, CR assumed that the marginal distributions shown in Table 1 are from known families. In particular, they assumed that *PL* and *H* are scaled-beta distributions, *C* is beta, and *O* is normally distributed. CR's parameter assumptions for each uncertainty are presented in Table 2.

With this information, CR proposed a single continuous joint probability density function (pdf), based on an NC, and discretized it using the Extended Pearson–Tukey (EPT) technique (Keefer and Bodily 1983,

Figure 3 Influence Diagram for Eagle Airline's Decision

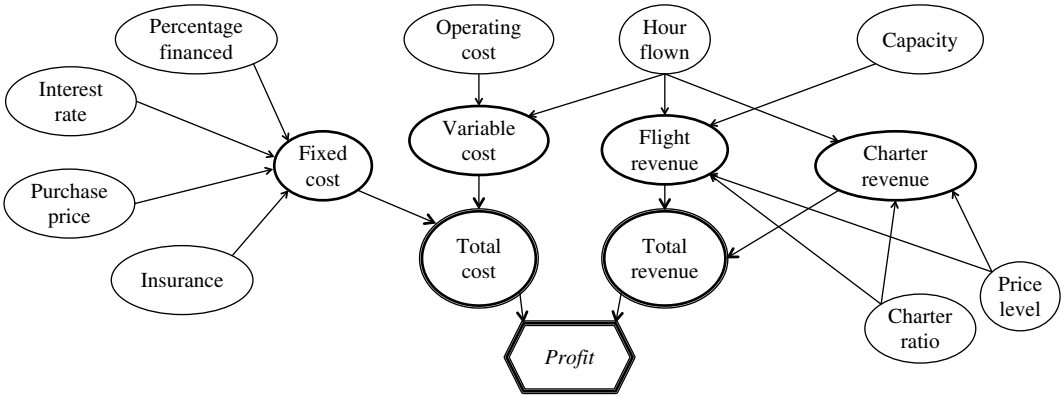

Pearson and Tukey 1965). The EPT technique weights the 0.05, 0.50, and 0.95 fractiles with probabilities of 0.185, 0.630, and 0.185, respectively. CR's discrete cumulative distribution function (cdf) for the Expand alternative is shown in Figure 4 as a solid black line. This figure should be compared to CR's "discrete approximation" in their Figure 5.

Because CR used the EPT technique, they fixed the probabilities for marginal and conditional distributions, as described above, and solved for the 0.05, 0.50, and 0.95 fractiles. In our simulation procedure, we fix the values and solve for the probabilities. This approach is helpful for comparing our procedure to an approximation such as maxent, which is not a function of values and instead solves for probabilities. Therefore, to better compare our procedure to that of CR, we have discretized their joint pdf by fixing the marginal values at the 0.05, 0.50, and 0.95 fractiles (using their pdf assumptions in Table 2) and then solving for probabilities using moment matching (see Appendix B). This discrete cdf is shown in Figure 4 as the solid gray line. Although the two approaches are not identical, the discretizations are very close. We use the moment matching cdf in the remainder of this paper.

One potential difficulty with CR's procedure, or that of Wang and Dyer (2012), is that it does not preserve the original pairwise correlation assessments. This occurs because the discretization with three points reduces the possible correlation range, producing a new correlation matrix bounded by $[-0.74, 0.74]$. Our approach, in contrast, preserves the assessed correlations. Of course, the expert would need to understand that the correlation range is not $[-1, 1]$ when they were assessing the rank correlation between discrete random variables with only three possible outcomes. Table 3 presents the rank correlation matrix implied by CR's discrete cdf (the gray line in Figure 4). See Appendix C for more detail.

Table 1 Ranges and Spearman Correlations for Critical Input Variables

	Fractile			Spearman correlations			
	Low	Base	High				
Uncertainty	0.10	0.50	0.90	*PL*	*H*	*C*	*O*
PL	\$95	\$100	\$108	1			
H	500	800	1,000	−0.50	1		
C	40%	50%	60%	−0.25	0.50	1	
O	\$230	\$245	\$260	0	0	0.25	1

Table 2 Marginal Distributions for Eagle Airlines

Uncertainty	Distribution	Parameters	Range
PL	Scaled beta	$\alpha = 9, \beta = 15$	[\$81.94, \$133.96]
H	Scaled beta	$\alpha = 4, \beta = 2$	[66.91, 1,135.26]
C	Beta	$\alpha = 20, \beta = 20$	[0, 1]
O	Normal	$\mu = 245, \sigma = 11.72$	$(-\infty, +\infty)$

Table 3 NC Implied Spearman Correlation Matrix

	PL	*H*	*C*	*O*
PL	0.74			
H	−0.38	0.74		
C	−0.19	0.38	0.74	
O	0	0	0.19	0.74

Figure 4 Eagle Airlines cdf, Under Original Discretization (Black) and New Discretization (Gray)

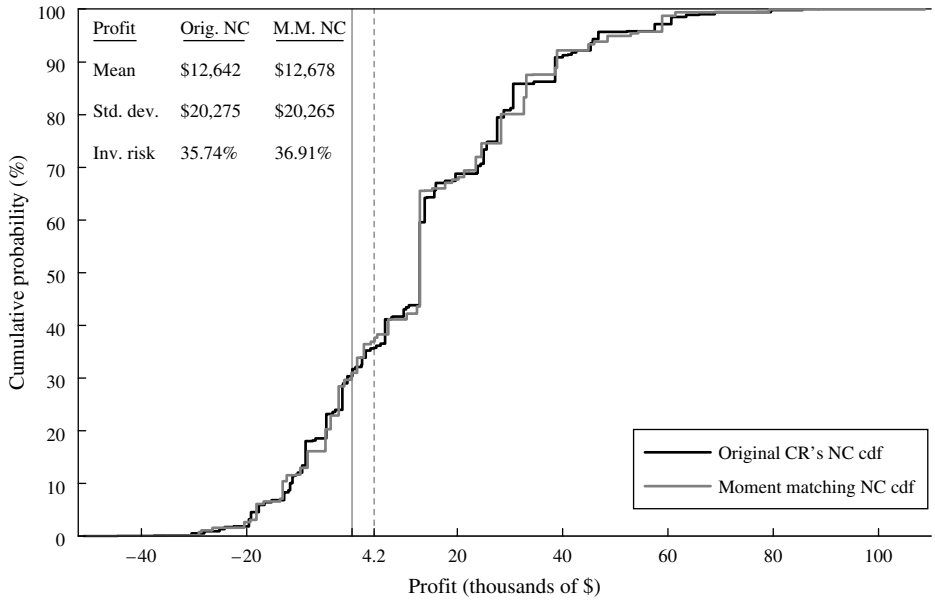

4. Application to Eagle Airlines Decision

In this section, we apply our JDSIM procedure to the Eagle Airlines case. We consider three information cases. The first case assumes we have information regarding only the marginal probabilities. The second case includes the previous marginal probabilities and adds information regarding the rank correlation between *PL* and *H*. The final case is equivalent to the original problem as presented by CR, and includes all the marginal assessments and pairwise correlations. To facilitate comparison of our results to those of CR, our JDSIM procedure uses the correlations presented in Table 3.

We begin by assuming that we have information regarding only the marginal assessments. To compare our procedure to that of CR, we also use the EPT technique. In addition to the 0.50 fractile, the EPT technique requires the 0.05 and 0.95 fractiles, which were not provided by CR. We estimate these fractiles using CR's distributional assumptions in Tables 1 and 2 and present the results in Table 4. We now assume that both the NC and JDSIM methods begin with Table 4. It is important to understand that this "preprocessing" is only done so that we can compare our procedure with CR. In practice, one would simply need to assess the information provided in Table 4.

Table 4 Fractiles Used in Eagle Airlines Example

	Fractile		
	Low (*l*)	Base (*b*)	High (*h*)
Uncertainty	0.05	0.5	0.95
PL ($)	93.47	100	110.05
H (hours)	432.92	800	1,053.60
C (%)	37.14	50	62.86
O ($)	225.72	245	264.28

4.1. Case 1: Given Information Regarding Marginals Alone

Under the NC procedure, we would use the marginal assessments provided in Table 4. We would next need to assume the marginal distributions belonged to a particular continuous family. This was done by CR yielding their assumptions in Table 2. Because we are assuming that dependence information is unavailable, it is unclear how to specify the correlation matrix. For the benefit of the comparison, and following common practice, we assume that all correlations are zero.

The JDSIM method, in contrast, does not require the specification of marginal pdf families or a correlation matrix. Rather, we form a polytope that contains all possible joint distributions matching the marginal assessments given in Table 4. The polytope describing these marginal assessments has 72 dimensions,

Figure 5 **Risk Profile Range Given Only Marginal Information, Minimum and Maximum Probability Bounds (Dashed), Theoretical Bounds (Solid), ASO (Black), and NC (Gray)**

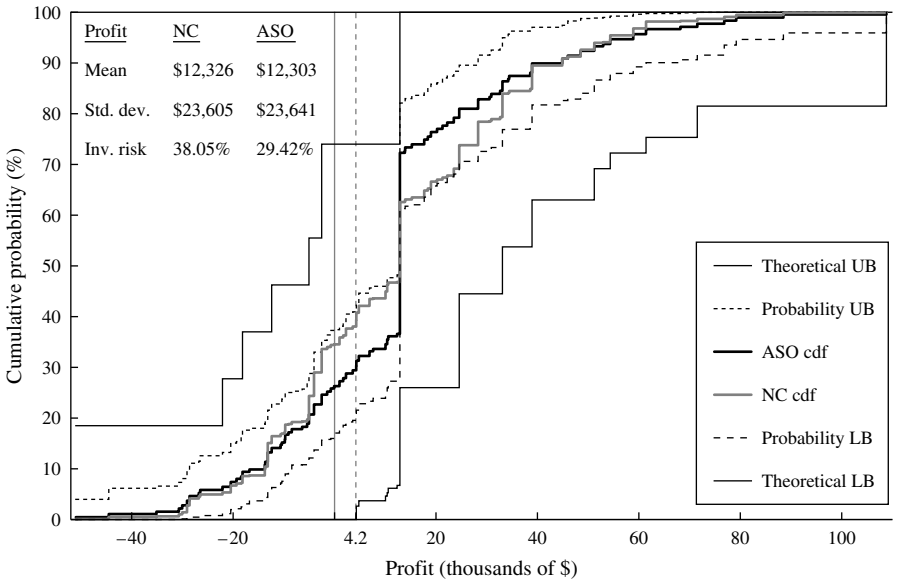

resulting from 81 joint probabilities (four random variables with three outcomes each), one constraint that requires the probabilities to sum to one, and eight constraints to match the marginal assessments ($81 - 1 - 8 = 72$).

The polytope $\mathbb{T}$ is defined using Equations (2a), (2b), and (3). Equations (2a) and (2b) constrain the joint probabilities $p_{\omega_k} \in \mathbf{p}$ to sum to one and to be nonnegative. Equation (3) selects subsets of the joint probabilities and constrains their sum to be equal to the marginal assessments. For example, if we order the random variables as (PL, H, C, O), each having values (l, b, h), there are 81 joint events. Using dot notation, $(h, \cdot, \cdot, \cdot)$ refers to the 27 joint events with PL equal to 110.05 (the 95th percentile). From the marginal assessments, we know that $p_{h,\cdot,\cdot,\cdot} = 0.185$, which defines Equation (6). Similar equations can be defined for the remaining 11 marginal assessments (12 in total). However, four of these constraints are redundant given Equation (2a), reducing the total number of linear constraints to nine.

$$p_{h,\cdot,\cdot,\cdot} = \sum_{i\in F}\sum_{j\in F}\sum_{k\in F} p_{h,i,j,k} = 0.185, \quad \forall F \equiv \{l, b, h\}. \quad (6)$$

We apply the JDSIM procedure to the polytope to create a discrete representation of $\mathbb{T}$ by sampling 10 million discrete joint distributions (run time of five hours using Mathematica 8 on an Intel central processing unit Q6700 at 2.67 GHz with 8 GB of random access memory), all of which are consistent with the information provided by CR. This sample size is more than sufficient to ensure uniform coverage of $\mathbb{T}$. For a full analysis of JDSIM's required sample size, we refer the reader to Montiel and Bickel (2012) and Montiel (2012).

We calculate the mean and standard deviation of profit for each sampled joint distribution. Additionally, we calculate the frequency with which the Expand alternative yields less than the Money Market (MM) threshold of \$4,200. We refer to this frequency as the "investment risk." Based on our 10 million distributions, we calculate frequency distributions for the mean profit, the standard deviation of profit, and the investment risk. Table 5 shows these percentiles along with their theoretical lower bound (LB) and upper bound (UB), which we describe shortly. This table should be compared to CR's Table 5.

The observed mean profit ranges from \$10,160 to \$14,340, with an average (μ) and standard deviation (σ) of \$12,303 and \$496, respectively. The expected profit under the NC is \$12,326. Our observed profit range and the percentiles closely match the results of CR's sensitivity results (see their Table 5).

Table 5 Percentiles for Mean Profit, Standard Deviation of Profit, and Investment Risks for JDSIM Joint Distributions Given Only Marginal Information

	Percentiles									Statistics	
	LB	0%	10%	25%	50%	75%	90%	100%	UB	μ	σ
Mean ($)	4,332	10,160	11,667	11,968	12,304	12,637	12,940	14,340	21,750	12,303	496
Std. dev. ($)	NA	17,300	21,750	22,613	23,576	24,552	25,456	29,580	NA	23,591	1,444
Inv. risk (%)	0.00	19.50	26.25	27.65	29.30	31.12	32.79	40.95	74.00	29.42	2.54

We refer to the 0th and 100th percentiles as "probability bounds" because there could exist cdfs in $\mathbb{T}$ that result in profits outside of this range. However, we did not observe them in 10 million samples. Because the minimum expected profit that we sampled was \$10,160, every simulated joint distribution had a mean profit greater than the value of the MM alternative. Thus, in this case, the assessment of probabilistic dependence or differing marginal distributions, which still match the assessments in Table 4, is very unlikely to change the recommendation that Eagle Airlines should expand (assuming they are risk neutral).

The standard deviations of our sampled cdfs ranged from \$17,300 to \$29,580, with an average of \$23,641. The standard deviation of profit under the NC is \$23,605. On the high end, our results closely match those of CR. However, the smallest standard deviations in our sample were larger than CR's. We conjecture that this result is related to differences in our discretization procedure and CR's marginal/copula assumptions. Referring back to Figure 4, we see that our discretization procedure (fixed values) results in a slightly wider cdf (longer tails) than CR's approach (fixed probabilities). Furthermore, their marginal distributions (see Table 2) are either normal or close to normal, implying that they have very thin tails. Likewise, CR modeled dependence with a normal copula, which also enforces thinner tails. JDSIM is not constrained by these assumptions and is therefore sampling from distributions that are most likely more spread and contain nonzero higher moments (e.g., skewness and kurtosis).

Table 5 indicates that investment risk, which averaged 29.42%, ranges from 19.50% to 40.95%. Although the Expand alternative's expected profit always exceeds the MM, there may be a large probability of underperforming this benchmark. This surprisingly large range is driven by the underlying dependence structure, which highlights the importance of modeling and assessing dependence. The NC investment risk is 38.05%. The most significant difference between the ASO and NC cdfs is at the level of individual fractiles—their first two moments are relatively close.

The LB and UB in Table 5 were derived from a linear program (LP) described in Appendix D. We provide these hard bounds for the mean profit and investment risk only. Determining the minimum and maximum possible standard deviation requires solving an NP-hard problem, and this was not attempted. The expected-profit LB is \$4,332, which is greater than the MM. Thus, it is impossible to generate a joint distribution matching the assessments in Table 4 that would underperform the MM investment.

The LB and UB are quite distant from the minimum (\$10,160) and maximum (\$14,340) expected profits. The joint distributions associated with these hard bounds contain many events with zero probability. For example, the joint distributions for the expected profit LB and UP are, respectively,

$$\{p_{l,h,l,h} = 0.185,\ p_{b,b,b,b} = 0.63,\ p_{h,l,h,l} = 0.185,\ 0 \text{ otherwise}\} \quad \text{and}$$

$$\{p_{l,l,l,h} = 0.185,\ p_{b,b,b,b} = 0.63,\ p_{h,h,h,l} = 0.185,\ 0 \text{ otherwise}\}.$$

These distributions, consisting mostly of zeros, are located at the vertices of the polytope. As such, they are geometrically extreme and unlikely to be sampled. They are also extreme from a dependence perspective, because they assume perfect dependence between the random variables. For example, under the minimum expected profit distribution, if PL is at its base value, then H, C, and O are certain to be at their base values as well.

This difference between the minimum and maximum sampled values (i.e., the probability bounds) and the theoretical bounds is explained by what we call the "sea urchin" effect (Appendix E). In high-dimension polytopes, the vertices become "thin" and comprise a very small portion of the total volume. Hence, JDSIM is unlikely to sample them. We do not believe this is a limitation of the sampling method. To the contrary, these distributions are extreme. If the underlying dependence was as strong as the distributions above require (e.g., perfect), we believe the expert would know this and could therefore express it as a constraint. Under these conditions, the JDSIM methodology would only sample distributions that included the expressed level of dependence.

The cdfs for this case are presented in Figure 5. The ASO cdf is the solid black line, and the independence cdf (based on an NC) is the solid gray line. The dotted lines are the minimum and maximum probability bounds that were sampled during our 10 million trials. These bounds are not individual cdfs, but represent the minimum (lower line) and maximum (upper line) cumulative probabilities that were sampled at each profit level. Likewise, the thin solid lines represent the theoretical minimum and maximum. These bounds were calculated using the LP described in Appendix D. All cdfs must fall within these latter bounds. The vertical dashed line denotes the MM value, and a vertical solid line denotes zero profit. The chance of underperforming MM matches the investment risk in Table 5.

We pause here to emphasize the scope and importance of our results. We have sampled 10 million joint distributions from the set of *all* discrete joint distributions matching the marginal constraints (Table 4). In other words, we have sampled from the set of all possible marginal distributions and dependence structures, rather than a set limited to marginals from particular families (e.g., beta) and whose dependence structure can be defined with a particular copula (e.g., normal). These 10 million joint distributions fall within the bounds denoted by the dotted lines. The (NC-based) independence cdf falls within these bounds, but is rather extreme (relative to the probability bounds) for profits between −\$3,000 and \$25,000. The ASO cdf might be thought of as being more representative of the set of possible joint distributions than the independence cdf. The ASO and the independence cdfs differ rather dramatically at a profit level of \$4,200, which is the MM benchmark.

4.2. Case 2: Given Information Regarding Marginals and One Pairwise Correlation

This section analyzes the case where the dependence structure is constrained by a single pairwise correlation. Specifically, we consider CR's implied correlation between PL and H, which is equal to -0.38 (see Table 3). We make no assumptions regarding the other five pairwise correlations. The truth set is generated using Equations (2a), (2b), (3), and (4a). As mentioned in §4.1, Equations (2a), (2b), and (3) ensure the sampled points are pmfs that match the marginal assessments. We add one more constraint (Equation (4a)) to fix the rank correlation between PL and H.

To illustrate Equation (4a), we describe the construction of one of the 81 coefficients for the joint events. Using the notation from §2.1, the 50th joint event corresponds to (b, h, b, b) and is described as $\omega_{50} = (PL = \$100, H = 1{,}053.6, C = 50\%, O = \$245)$. Equations (4a)–(4d) then yield

$$\begin{aligned}\mathbf{B}_{\omega_{50}} &= [I_{\omega_{50}}(PL) \times I_{\omega_{50}}(H)] = [p_{50}^{PL+}, p_{50}^{PL-}] \times [p_{50}^{H+}, p_{50}^{H-}] \\ &= [0.815, 0.185] \times [1.0, 0.815],\end{aligned}$$

$$\begin{aligned}&\frac{\mathbf{V}_{(xy)^2}[\mathbf{B}_{\omega_{50}}]}{q_{\omega_{50}^+(PL)} q_{\omega_{50}^+(H)}} \\ &= \frac{(p_{50}^{PL+}p_{50}^{H+})^2 - (p_{50}^{PL+}p_{50}^{H-})^2 - (p_{50}^{PL-}p_{50}^{H+})^2 + (p_{50}^{PL-}p_{50}^{H-})^2}{P(PL=100)P(H=1{,}053.6)} \\ &= ((0.815 \cdot 1.0)^2 - (0.815 \cdot 0.815)^2 - (0.185 \cdot 1.0)^2 \\ &\qquad + (0.185 \cdot 0.815)^2) \cdot (0.63 \cdot 0.185)^{-1} \\ &= 1.815.\end{aligned}$$

Calculating similar coefficients for all 81 joint events defines Equation (4a) and yields

$$\begin{aligned}&0.0342p_{l,l,\cdot,\cdot} + 0.185p_{l,b,\cdot,\cdot} + 0.3358p_{l,h,\cdot,\cdot} + 0.185p_{b,l,\cdot,\cdot} \\ &\quad + p_{b,b,\cdot,\cdot} + 1.815p_{b,h,\cdot,\cdot} + 0.3358p_{h,l,\cdot,\cdot} + 1.815p_{h,b,\cdot,\cdot} \\ &\quad + 3.2942p_{h,h,\cdot,\cdot} = \frac{\rho_{PL,H} + 3}{3}.\end{aligned}$$

The maximum correlation occurs at $p_{l,b,\cdot,\cdot} = p_{l,h,\cdot,\cdot} = p_{b,l,\cdot,\cdot} = p_{b,h,\cdot,\cdot} = p_{h,l,\cdot,\cdot} = p_{h,b,\cdot,\cdot} = 0$, $p_{l,l,\cdot,\cdot} = 0.185$, $p_{b,b,\cdot,\cdot} = 0.63$, $p_{h,h,\cdot,\cdot} = 0.185$ and has a value of 0.74, as shown in Table 3.

Table 6 **Percentiles for Mean Profit, Standard Deviation of Profit, and Investment Risks for JDSIM Joint Distributions Given Marginal Information and One Pairwise Correlation Coefficient**

	Percentiles									Statistics	
	LB	0%	10%	25%	50%	75%	90%	100%	UB	μ	σ
Mean ($)	4,877	9,215	10,376	10,641	10,919	11,198	11,441	12,570	16,691	10,916	414
Std. dev. ($)	NA	16,500	19,820	20,499	21,269	22,062	22,833	26,180	NA	21,296	1,174
Inv. risk (%)	0.57	20.50	25.87	27.40	29.25	31.17	32.99	42.20	73.43	29.36	2.78

We apply the JDSIM procedure to the new polytope and create a discrete representation of the new truth set by sampling 10 million possible joint distributions. Each sampled distribution has marginals equal to 0.185, 0.63, and 0.185 of (l, b, h), respectively, and rank correlation $\rho_{PL,H} = -0.38$. Table 6 summarizes our results.

The sampled mean profit ranges from \$9,215 to \$12,570, with an average value of \$10,916 and a standard deviation of \$414. The NC expected profit is also \$10,916. The distribution of the mean profit shows that under the new information, the Expand alternative is less attractive than before. This occurs because the correlation between PL and H is negative; higher prices result in fewer hours being flown. However, purchasing the plane is still more attractive than investing in the money market, even at the theoretical bounds (LB and UB). The standard deviations are slightly lower than in Case 1 because we have introduced negative dependence between PL and H. The investment risk now ranges from 20.50% to 42.20%, with an average of 29.36%.

The cdfs for this case are presented in Figure 6. The ASO cdf assumes that $\rho_{PL,H} = -0.38$ and all other correlations are unspecified. The NC cdf assumes that $\rho_{PL,H} = -0.38$ and all other correlations are zero. As in Case 1, the NC cdf is near the probability bounds for profits of −\$3,000 to \$25,000. Again, the ASO seems to be more representative than the NC of the set of possible distributions.

4.3. Case 3: Given Information Regarding Marginals and All Pairwise Correlations

In this section, we adopt all of the information provided by CR and used in their NC approach. Specifically, we use the marginal assessments from the EPT discretization, given in Table 4, and the implied correlations from Table 3. The implied

Figure 6 **Risk Profile Range Given Marginal Information and One Pairwise Correlation Coefficient, Minimum and Maximum Probability Bounds (Dashed), Theoretical Bounds (Solid), ASO (Black), and NC (Gray)**

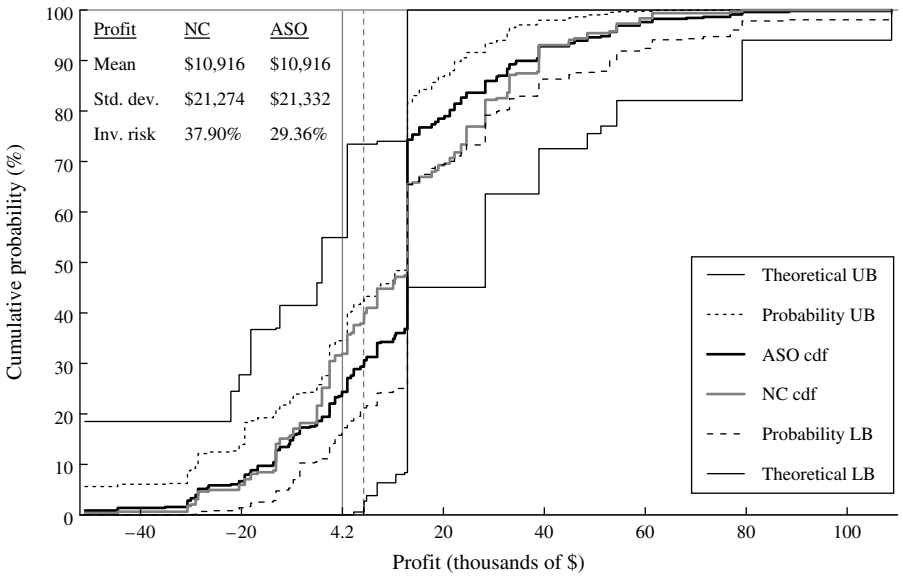

Table 7 Percentiles for Mean Profit, Standard Deviation of Profit, and Investment Risks for JDSIM Joint Distributions Given Marginal Information and all Pairwise Correlation Coefficients

	Percentiles									Statistics	
	LB	0%	10%	25%	50%	75%	90%	100%	UB	μ	σ
Mean ($)	12,049	12,448	12,583	12,620	12,662	12,704	12,741	12,910	13,271	12,662	62
Std. dev. ($)	NA	18,530	19,767	20,063	20,400	20,750	21,051	22,280	NA	20,404	499
Inv. risk (%)	9.55	18.45	24.63	25.98	27.54	29.18	30.76	36.50	63.72	27.64	2.36

correlations are used to make the comparison to CR as fair as possible. The new polytope is defined using Equations (2a), (2b), (3), and (4a), as illustrated in §§4.1 and 4.2. To the previous 10 constraints (and the nonnegativity constraints), we add five new constraints to fix the values of all the pairwise correlations, defining a 66-dimensional polytope.

Table 7 displays a summary of our 10 million samples of the new polytope using JDSIM. The additional constraints have significantly affected the mean profit distribution. The minimum and maximum sampled mean profits are now \$12,448 and \$12,910, respectively, with an average of \$12,662 and a standard deviation of \$62. The NC expected profit is \$12,678, which matches the value given in Figure 4. Additionally, the difference between the theoretical mean profit UB and LB is only \$1,222, which is considerably less than in our previous cases. What little difference there is between mean profits is due to dependence in the joint distribution that cannot be described by pairwise correlations.

The new distribution of the standard deviation of profit ranges from \$18,530 to \$22,280, with an average \$20,404. The distribution of the investment risk has been shifted toward lower values (although the LB has increased), with a new range from 18.45% to 36.50%. The average investment risk is now 27.64%.

The bounds for the cdfs when all pairwise correlations are known are shown in Figure 7. Both the probability and the absolute boundaries are narrower than before. CR's NC cdf falls slightly outside of the probability bounds for profit values of $-\$2{,}000$ to \$25,000. This suggests that the NC approach, which specifies a single joint distribution, may not generate an approximation that is representative of the set of all distributions matching the assessed information.

Figure 7 Risk Profile Range Given Marginal Information and All Pairwise Correlation Coefficients, Minimum and Maximum Probability Bounds (Dashed), Theoretical Bounds (Solid), ASO (Black), and NC (Gray)

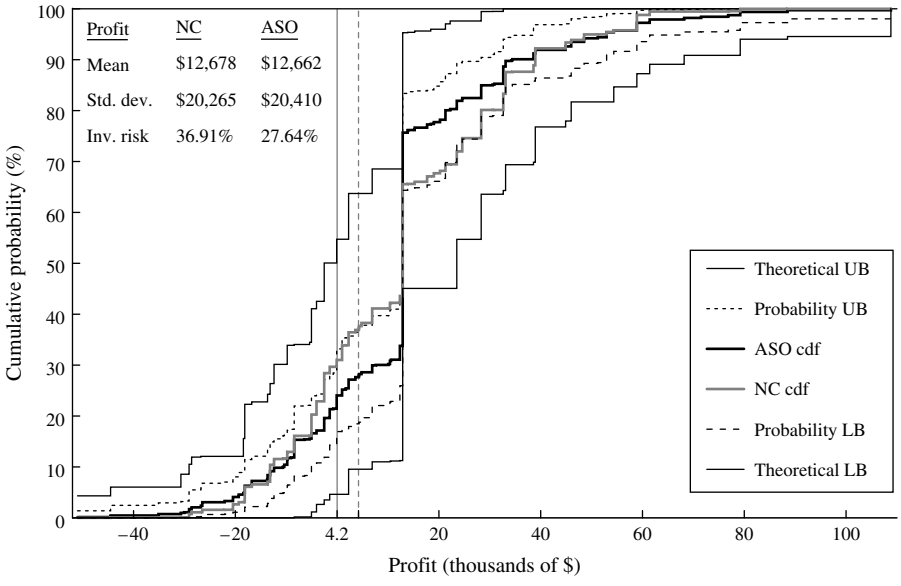

We conjecture that the extreme behavior of the NC with respect to the probability bounds is related to the structure provided by the normal copula. The normal pdf has maximum entropy for a given mean and standard deviation. We suspect that joint distributions formed with a normal copula are also high in entropy. Indeed, in our case, CR's NC cdf and the (not shown) maximum-entropy cdf (given marginal and all pairwise correlations) are very close to each other, with a maximum absolute difference among the probabilities of the joint events of 0.0037, whereas the corresponding difference between NC and ASO is 0.1992. A maxent joint distribution based on marginals and pairwise correlations will enforce higher-order dependencies that are as close to independence as possible. This cdf will then tend to be an extreme point within our truth set. As a simple illustration, assume two identical binary random variables with marginals of $\{0.9, 0.1\}$ and unknown correlation. With this information, all the possible distributions are a convex combination of $\{0.9, 0, 0, 0.1\}$ and $\{0.8, 0.1, 0.1, 0\}$. Hence, $\mathbb{T}$ forms a line section with center at $\{0.85, 0.05, 0.05, 0.05\}$, whereas maxent is located at $\{0.81, 0.09, 0.09, 0.01\}$, close to the second extreme point.

4.4. Comparing the Three Information Cases

Figure 8, (a)–(c), compares the pdfs (frequencies) of our sampled expected profits, standard deviations, and investment risk, respectively. The distribution for Case 1, using only marginal information, is presented as the dotted line filled in white. Case 2, using marginal information and one pairwise correlation coefficient, is presented as the dashed line filled in gray. Finally, Case 3, with all marginal information and pairwise correlation assessments, is presented in a solid line filled in black. The vertical lines correspond to the probability bounds for each case mark in dotted (Case 1), dashed (Case 2), and solid lines (Case 3).

The range of outcomes for Case 1 (only marginals) stems from our having not constrained marginal families or the dependence structure. The addition of a negative correlation between PL and H, in Case 2, shifted the set of possible profits to the left and narrowed it somewhat. The specification of all pairwise correlations, in Case 3, constrained the set considerably. The variability that does exist is related to our marginals' not having been based on known families and that higher-order dependencies (beyond pairwise) were not fixed. This indicates that assessing

Figure 8 **Sampled Distributions for Mean Profit, Standard Deviation of Profit, and Investment Risk Given Marginals Only (White), Marginals and One Pairwise Correlation (Gray), and Marginals and All Pairwise Correlations (Black)**

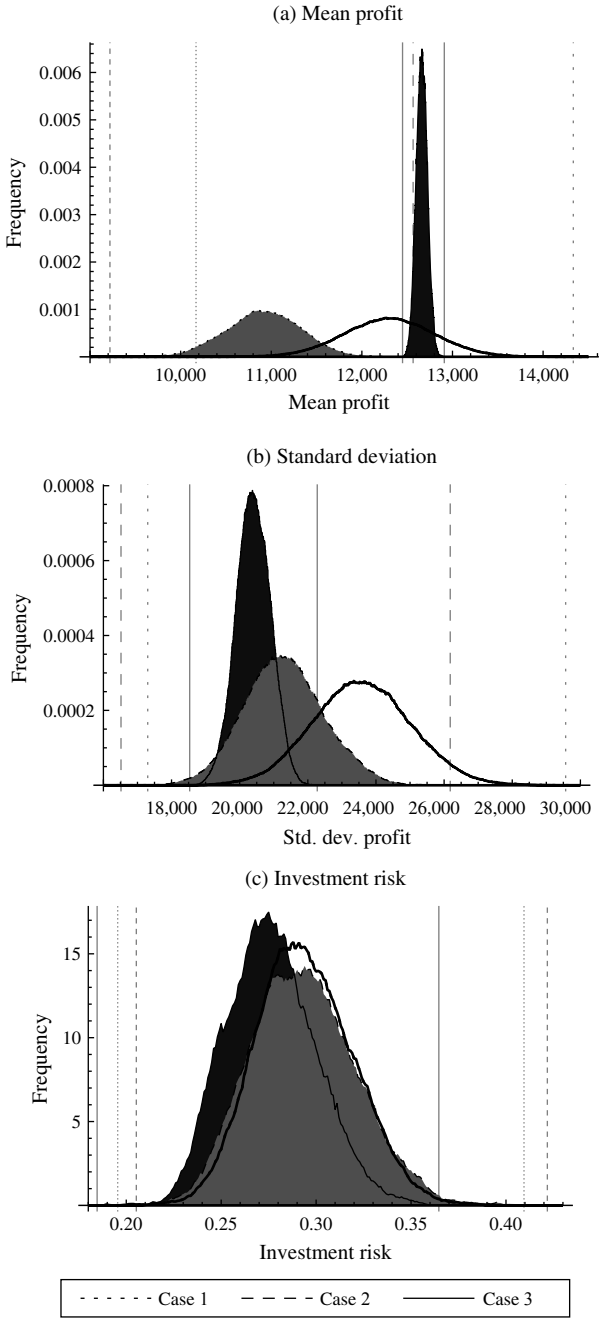

these higher-order distributions (e.g., all three-way assessments) will not improve the decision.

The investment-risk distributions show less sensitivity to the dependence structure. Although additional constraints had a significant impact on the distribution of expected profit and the standard deviation of profit, the probability of it being less than \$4,200 has not changed significantly.

5. Conclusions

Both the JDSIM and the NC approaches provide methods to model probabilities and decisions when only partial probabilistic information is available. The NC approach requires (1) the assumption of marginal distributions (e.g., Table 2) that fit the provided assessments (e.g., Table 4) and (2) a copula to specify a single joint probability distribution. These two assumptions specify a single joint distribution. JDSIM, in contrast, explores the set of all joint distributions that match the available information.

JDSIM provides a flexible and powerful tool to analyze stochastic decision models when the joint distribution is incompletely specified. The methodology is easy to implement, develops a collection of joint distributions, and represents a significant extension to previous approximation models such as the copula-based approach illustrated by CR. We demonstrated the JDSIM procedure with a canonical example based on marginal and pairwise rank correlation coefficients. The methodology can be extended to more than four random variables, to random variables with more than three possible outcomes, and to higher-order conditioning such as three-way assessments.

On average, the profit joint distributions produced by JDSIM resulted in expected values and standard deviations similar to those of NC. The primary difference, in the case examined here, seems to be differing estimates for particular cumulative probabilities. For example, the NC cdf produced cumulative probabilities for midrange profits that were extreme relative to our sample. This is potentially important in the Eagle Airlines case because this profit range included the value of the competing alternative. Thus, the two methods might produce very different estimates of investment risk (the probability of under performing the competing alternative). This being said, more research needs to be done to better understand if it is possible to faithfully represent the JDSIM sample with a single joint distribution across a range of applications.

JDSIM's strength is also a potential weakness, because the decision is not valued or made under a single distribution, but rather under thousands (possibly millions) of feasible distributions. NC provides a single, approximate distribution, but, as discussed above, our results suggest that this approximation may not be representative of the set of possible joint distributions. The accuracy of the normal copula approach is an open question, but one that could be addressed by comparing it to the JDSIM results.

The information provided by this new simulation procedure provides insight regarding the shape of the truth set. At this point, we do not claim to know the likelihood of the distributions in the sampled collection. However, we can clearly state that assuming independence in scenarios with incomplete or unknown information provides approximations that are extreme relative to the other distributions in the truth set. This provides yet another example of the importance of not ignoring dependence.

Future research will use JDSIM to quantify the accuracy of common approximation methods such as maxent. Although maxent is commonly used, its accuracy has not been studied carefully. The results presented in this paper suggest that maxent is a rather extreme assumption. For example, if a correlation is not specified, maxent assumes it is zero. In this sense, maxent may not be representative of the set of all distributions matching a given set of constraints on the underlying distributions.

Electronic Companion

An electronic companion to this paper is available as part of the online version at http://dx.doi.org/10.1287/deca.1120.0252.

Acknowledgments

The authors thank Tianyang Wang, the associate editor, and two anonymous referees for their helpful comments and suggestions on a draft of this paper. This work was supported by the National Science Foundation under J. E. Bickel's CAREER grant [Grant SES-0954371].

Appendix A. Spearman's Correlation Derivation

In this addendum, we derive the Spearman's correlation (Equation (4a)) from basic principles. Following Nelsen (1991, p. 55; 2005, p. 170) we define Spearman's rank correlation for (V_i, V_j) to be the Pearson's product moment correlation for $(U, V) = (F(V_i), F(V_j))$. Thus,

$$\rho^r_{V_i,V_j} = \frac{\mathrm{Cov}(U,V)}{\sqrt{\mathrm{Var}(U)\cdot\mathrm{Var}(V)}}. \tag{A1}$$

Because U and V are uniform with mean 1/2 and variance 1/12, we have

$$\begin{aligned}\rho^r_{V_i,V_j} &= \frac{E(UV)-E(U)E(V)}{\sqrt{\mathrm{Var}(U)\cdot\mathrm{Var}(V)}} = \frac{E(UV)-1/4}{1/12}\\ &= 12\cdot E(UV)-3.\end{aligned} \tag{A2}$$

Nelsen (1991, p. 55) evaluates $E(UV)$ using a copula, where $dC(u,v) = u\cdot v\cdot c(u,v)$:

$$\begin{aligned}\rho^r_{V_i,V_j} &= 12\int_0^1\int_0^1 u\cdot v\cdot dC(u,v)-3\\ &= 12\int_0^1\int_0^1 u\cdot v\cdot c(u,v)\,du\,dv-3.\end{aligned} \tag{A3}$$

Equation (A3) is also given by MacKenzie (1994, p. 14). The following step uses the fact that $\int_0^1 x\,dx = \int_0^\alpha x\,dx + \int_\alpha^1 x\,dx,\ \forall\,\alpha\in[0,1]$, where the functions $p_k^-(V_i)$ and $p_k^+(V_i)$ generate a partition of the range of $F(V_i)$ over the $[0,1]$ interval. The total number of elements in the sum is equal to the cardinality of $\mathbb{U}$ and is indexed by ω_k:

$$\begin{aligned}\rho^r_{V_i,V_j} &= 12\int_0^1\int_0^1 u\cdot v\cdot c(u,v)\,du\,dv-3\\ &= 12\sum_{\omega_k\in\mathbb{U}}\int_{p_k^-(V_i)}^{p_k^+(V_i)}\int_{p_k^-(V_j)}^{p_k^+(V_j)} u\cdot v\cdot c(u,v)\,du\,dv-3.\end{aligned} \tag{A4}$$

Equation (A4) appears in MacKenzie (1994, p. 14), but under the restriction that the $[0,1]$ interval is divided into equal segments. Here, we allow for unequal segments to account for nonuniform marginals.

Recall that $p_k^+(V_i)$ and $p_k^-(V_i)$ are constructed with the marginal information, which we assume has been provided, and represents points in the cumulative marginal distribution $F(V_i)$. These functions define the intervals $I_{\omega_k}(V_i)$ and $I_{\omega_k}(V_j)$ for every k defining a grid (possibly uneven). We illustrate the partition with an example provided in Figure A.1, where the section $I_{\omega_6}(V_i)\times I_{\omega_6}(V_j) = [p_6^+(V_1), p_6^-(V_1)]\times[p_6^+(V_2), p_6^-(V_2)]$ is shaded, assuming the marginal distributions of V_i and V_j are $P(V_1=0)=0.2$, $P(V_1=1)=0.4$, $P(V_1=2)=0.4$, and $P(V_2=0)=0.3$, $P(V_2=1)=0.3$, $P(V_2=2)=0.2$, $P(V_2=3)=0.2$. The section is $[(0.2+0.4), 0.2]\times[(0.3+0.3), 0.3]$.

Once the partition is created, we define $c(u,v)$ to be uniform inside each partition. Thus, by choosing $c(u,v) = c(\omega_k(V_i), \omega_k(V_j))$ constant for each section on the grid,

Figure A.1 Grid Generated by the Interval $I_{\omega_k}(V_i)$

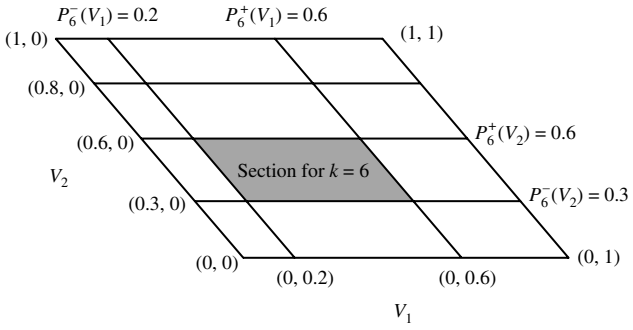

where $\omega_k(V_i)$ is the marginal realization of V_i in the joint realization ω_k, we can take it out of the integral, which yields

$$\rho^r_{V_i,V_j} = 12\sum_{\omega_k\in\mathbb{U}}\int_{p_k^-(V_i)}^{p_k^+(V_i)}\int_{p_k^-(V_j)}^{p_k^+(V_j)} u\cdot v\cdot c(u,v)\,du\,dv-3 \tag{A5a}$$

$$= 12\sum_{\omega_k\in\mathbb{U}} c(\omega_k(V_i),\omega_k(V_j))\cdot\int_{p_k^-(V_i)}^{p_k^+(V_i)}\int_{p_k^-(V_j)}^{p_k^+(V_j)} u\cdot v\,du\,dv-3. \tag{A5b}$$

Equations (A5a) and (A5b) are a generalization of Equation (3.9) of MacKenzie (1994, p. 14), which was derived under the restriction that the $[0,1]$ interval is divided into equal segments. We now evaluate the integrals and rearrange terms to make the equation more compact:

$$\begin{aligned}\rho^r_{V_i,V_j} = \frac{12}{4}\sum_{\omega_k\in\mathbb{U}} c(\omega_k(V_i),\omega_k(V_j))[&[p_k^+(V_i)p_k^+(V_j)]^2\\ &-[p_k^+(V_i)p_k^-(V_j)]^2-[p_k^-(V_i)p_k^+(V_j)]^2\\ &+[p_k^-(V_i)p_k^-(V_j)]^2]-3.\end{aligned} \tag{A6}$$

Nelsen (2005, p. 8) defines the *H-volume* as

$$\begin{aligned}&\mathbf{V}_{x^2*y^2}[I_{\omega_k}(V_i)\times I_{\omega_k}(V_j)]\\ &\quad=[p_k^+(V_i)p_k^+(V_j)]^2-[p_k^+(V_i)p_k^-(V_j)]^2\\ &\qquad-[p_k^-(V_i)p_k^+(V_j)]^2+[p_k^-(V_i)p_k^-(V_j)]^2.\end{aligned} \tag{A7}$$

Substituting Equation (A7) into Equation (A6), we get Equation (A8):

$$\rho^r_{V_i,V_j} = 3\sum_{\omega_k\in\mathbb{U}} c(\omega_k(V_i),\omega_k(V_j))\mathbf{V}_{x^2*y^2}[I_{\omega_k}(V_i)\times I_{\omega_k}(V_j)]-3. \tag{A8}$$

We can interpret the probability of each part of the grid as the volume assigned, where $q_{\omega_k^+(V_i)}$ and $q_{\omega_k^+(V_j)}$ are the length and width (given by the marginals of V_i and V_j), respectively, and $c(\omega_k(V_i),\omega_k(V_j))$ is the height of each subsection, as shown in Figure A.2:

$$c(\omega_k(V_i),\omega_k(V_j)) = \frac{p_{\omega_k}}{q_{\omega_k^+(V_i)}\cdot q_{\omega_k^+(V_j)}}. \tag{A9}$$

Figure A.2 $c(\omega_k(V_i), \omega_k(V_j))$ **Describes the Height of the Section** k

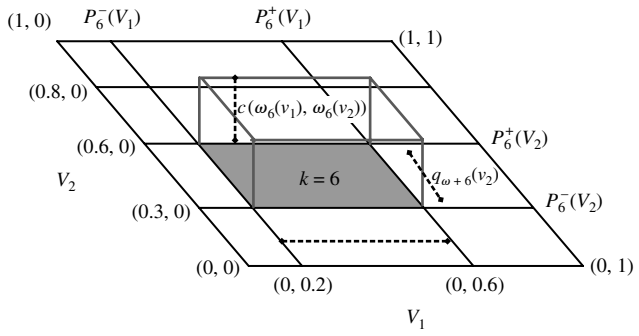

Substituting Equation (A9) into Equation (A8), we obtain Equation (A10):

$$\rho^r_{V_i, V_j} = 3 \sum_{\omega_k \in \mathbb{U}} p_{\omega_k} \frac{\mathbf{V}_{x^2 * y^2}[I_{\omega_k}(V_i) \times I_{\omega_k}(V_j)]}{q_{\omega_k^+(V_i)} \cdot q_{\omega_k^+(V_j)}} - 3. \quad \text{(A10)}$$

We define the parameter $\gamma^{(i,j)}_{\omega_k}$ as

$$\gamma^{(i,j)}_{\omega_k} = \frac{\mathbf{V}_{(xy)^2}[I_{\omega_k}(V_i) \times I_{\omega_k}(V_j)]}{q_{\omega_k^+(V_i)} \cdot q_{\omega_k^+(V_j)}} \quad \forall\, \omega_k \in \mathbb{U} \text{ and } i, j \in \mathbb{V}. \quad \text{(A11)}$$

Given the marginals of V_i and V_j, the parameter $\gamma^{(i,j)}_{\omega_k}$ is a known constant for every subindex k, where $q_{\omega_k^+(V_i)} = p_k^+(V_i) - p_k^-(V_i)$. Finally, substituting Equation (A11) into Equation (A10), we get Equation (A12):

$$\sum_{\omega_k \in \mathbb{U}} \gamma^{(i,j)}_{\omega_k} p_{\omega_k} = \frac{\rho_{i,j} + 3}{3} \quad \forall\, i, j \in \mathbb{V}. \quad \text{(A12)}$$

Spearman's rank correlation is then the weighed sum of the probabilities, where the weights are constants defined by the marginal probabilities of V_i and V_j. Therefore, the Spearman's rank correlation (Equation (A12)) is linear in the probabilities and can be expressed as linear equalities.

Appendix B. Moment Matching Discretization Procedure

CR's procedure uses the EPT technique to discretize their continuous joint distribution. Specifically, CR fixed probabilities and then solved for conditional fractiles. This approach is difficult to compare to the JDSIM procedure, which fixes values and solves for probabilities. To facilitate comparison, we use a different discretization based on moment matching. We start by discretizing the marginal distributions using the EPT technique and fix the values of the 0.05, 0.50, and 0.95 fractiles for all uncertainties. After discretizing the marginals, we proceed to discretize the conditional distributions using moment matching to find the respective probabilities (Smith 1993, Bickel et al. 2011).

The joint probability distribution can be decomposed using Equation (B1):

$$P(PL, H, C, O) = P(PL) \cdot P(H \mid PL) \cdot P(C \mid PL, H) \cdot P(O \mid PL, H, C). \quad \text{(B1)}$$

We start by discretizing $P(PL)$ using EPT and the values of the 0.05, 0.50, and 0.95 fractiles with outcomes \$93.47, \$100.00, and \$110.05, respectively. For these values, we define the probabilities p_l^{PL}, p_b^{PL}, and p_h^{PL} as 0.185, 0.63, and 0.185, respectively. Next, we discretize $P(H \mid PL = \$100.00)$ using the fixed values $\{432.92, 800, 1{,}053.60\}$ for H and use moment matching to find the correct probabilities $p^H_{l|b}$, $p^H_{b|b}$, and $p^H_{h|b}$. To completely discretize $H \mid PL$, we solve Equations (B2a), (B2b), and (B2c) for the three possible discrete outcomes of PL:

$$p^H_{l|b} + p^H_{b|b} + p^H_{h|b} = 1, \quad \text{(B2a)}$$

$$432.92 \cdot p^H_{l|b} + 800.00 \cdot p^H_{b|b} + 1{,}053.60 \cdot p^H_{h|b} = E[H \mid PL], \quad \text{(B2b)}$$

$$(432.92)^2 \cdot p^H_{l|b} + (800.00)^2 \cdot p^H_{b|b} + (1{,}053.60)^2 \cdot p^H_{h|b} = E[H^2 \mid PL]. \quad \text{(B2c)}$$

We discretize $P(C \mid PL, H)$ using equivalent equations matching $E[C \mid PL, H]$ and $E[C^2 \mid PL, H]$ and equivalent coefficients based on the fixed values for C to define $p^C_{l|\ldots}$, $p^C_{b|\ldots}$, and $p^C_{h|\ldots}$. The complete discretization of $P(C \mid PL, H)$ requires solving a total of nine moment matching problems, one for each joint outcome of $\{PL, H\}$. Finally, a similar procedure is applied to $P(O \mid PL, H, C)$, solving a total of 27 moment matching problems. After discretizing all 39 conditional distributions, we apply Equation (B3) as follows:

$$P(PL = l, H = b, C = h, O = b) = p_l^{PL} \cdot p^H_{b|l} \cdot p^C_{h|l,b} \cdot p^O_{b|l,b,h}. \quad \text{(B3)}$$

This alternative discretization fixes the values of the variables and models the probabilistic dependence using the probabilities of the joint events, which enables comparison our approach with CR. As shown in Figure 4, the two discretizations are very close.

Appendix C. Rank Correlation Range in Discrete Distributions

Typically, the rank correlation $\rho_{X,Y}$ between two random variables X, Y is perceived to be $-1 \le \rho_{X,Y} \le 1$, where the correlation between a variable and itself is defined with the maximum degree of association $\rho_{X,X} = 1$. However, the same concept only applies to discrete distributions when the number of discrete points tends to infinity. For most discrete distributions, $\rho_{X,Y}$ is bounded by a scalar $|a_{\hat{m}}| < 1$. For example, when X and Y have each $\hat{m}$ equally likely realizations, MacKenzie (1994) proved that $a_{\hat{m}} = 1 - 1/\hat{m}^2$. Then, the rank correlation is bounded by $-1 + 1/\hat{m}^2 \le \rho_{X,Y} \le 1 - 1/\hat{m}^2$, and as the number of realizations increases, $\lim_{\hat{m}\to\infty} |a_{\hat{m}}| = 1$. Nešlehová (2007) also found similar behavior for more general bounds where X and Y have arbitrary marginals.

As an illustration of this fact, recall that the maximum association dictates that $P(Y = y_i \mid X = x_i) = 1$ for every i. For example, in §4.2 we calculate the maximum $\rho_{PL,H}$ by assigning joint probabilities such that $P(PL = l \mid H = l) = P(PL = b \mid H = b) = P(PL = h \mid H = h) = 1$, which results in

$p_{l,l,\cdot,\cdot} = 0.185$, $p_{b,b,\cdot,\cdot} = 0.63$, $p_{h,h,\cdot,\cdot} = 0.185$, with all other probabilities equal to zero. Then, using Equation (4a) and as shown in §4.2, we can calculate that the maximum correlation possible is $\sup \rho_{PL,H} = 0.74$. Given that the rank correlation uses $P(X)$ instead of X, and that $P(PL) = P(H)$ in distribution, we have that $\rho_{PL,PL} = \sup \rho_{PL,H} = 0.74$, as shown in Table 3.

Appendix D. Absolute Bounds for Risk Profiles

Given the system of linear equations $\mathbf{Ap} = \mathbf{b}$, $\forall\, \mathbf{p} \geq 0$, where $\mathbf{A}$ is the matrix of coefficients of Equations (2a), (2b), (3), and (4a), and $\mathbf{b}$ represents the expert assessments, the decision variable $\mathbf{p}$ has 81 elements, one for each joint outcome of the cdf, and each joint outcome has a corresponding profit $\mathbf{v} = (v_1, v_2, \ldots, v_{81})$. Then, for an arbitrary profit u, the LB and UB of the cdf at u are calculated using the indicator function $\mathbf{1}_{\leq u}(v_i) = 1$ if $v_i \leq u$ and 0 otherwise.

The objective function $\mathbf{c}_u\mathbf{p}$, where $\mathbf{c}_u = (\mathbf{1}_{\leq u}(v_1), \mathbf{1}_{\leq u}(v_2), \ldots, \mathbf{1}_{\leq u}(v_{81}))$ is used to find the cdf with the min (max) cumulative probability of the random profit X been less than a value u, in other words, min (max) $P(X \leq u)$. Then, for any u, the lower (upper) bound can be calculated with Equation (D1):

$$\begin{aligned} &\min\,(\max) \quad \mathbf{c}_u\mathbf{p} \\ &\text{s.t.} \quad \mathbf{Ap} = \mathbf{b} \quad \forall\, \mathbf{p} \geq 0. \end{aligned} \tag{D1}$$

To produce a complete risk profile LB (UB), we need to solve Equation (D1) for $u = v_1$ to $u = v_{81}$. The value of the objective function for each of the 81 LPs produces the min (max) absolute bound. By selecting $\mathbf{c}_u = \mathbf{v}$, the same LP provide the theoretical lower (upper) bounds for the mean profits.

Appendix E. The Sea Urchin Effect: Volume in High-Dimension Polytopes

The description of the n-content (the volume in n dimensions) of a body in high dimensions is often unintuitive. Although the volume is uniformly distributed in the polytope, it may appear to be more concentrated in specific areas of its interior. We call this the sea urchin effect (after Johannes Kepler's naming the dodecahedron the *echinus*, which is Latin for sea urchin). Jimenez and Landgrebe (1998) described this behavior for several geometric bodies. However, we are interested only in the description of the unit simplex.

To observe the dispersion of the volume over $\mathbb{T}$, we create a partition of an unconstrained polytope (a unit simplex), slicing it horizontally from a corner to its base along the height (Figure E.1(a)).

We generate 1,000 sections ($S = 1{,}000$) and enumerate them starting with the section closest to the vertex. For each section, we measure the volume $\text{Vol}(\mathbb{T}_i)$ and take the proportions $Pr_i = \text{Vol}(\mathbb{T}_i)/\text{Vol}(\mathbb{T})$ for $i = 1, \ldots, 1{,}000$. If we take N samples, the number of samples in section i should be $N * Pr_i$. Equation (E1) describes the volume of the ith section (Figure E.1(b)). This section is generated by a single cut of $\mathbb{T}$ perpendicular to its height (H) at a distance $(i/S)H$, where S is the number of parts in the partition:

$$\sum_{k=1}^{i} \text{Vol}(\mathbb{T}_k) = \left(\frac{i}{S}\right)^n \cdot \frac{\sqrt{n+1}}{n!}, \quad \forall\, i = 1, \ldots, S. \tag{E1}$$

We illustrate the dispersion of volume in $\mathbb{T}$ by plotting the proportion of volume in each section for three scenarios using one, two, and four random variables with three possible outcomes each (Figure E.1(c)). The dimensions of the polytopes are $n = 2, 8$, and 80 and are shaded light gray, dark gray, and black, respectively. The concentration of the volume closer to the vertices decays rapidly with n.

Adding more dimensions increases the set of joint distributions that match a set of information. However, the sample taken by JDSIM is more concentrated. This apparent paradox is resolved by observing that even though $\mathbb{T}$

Figure E.1 Partition of a Polytope and Respective Volume Proportions for Three Scenarios

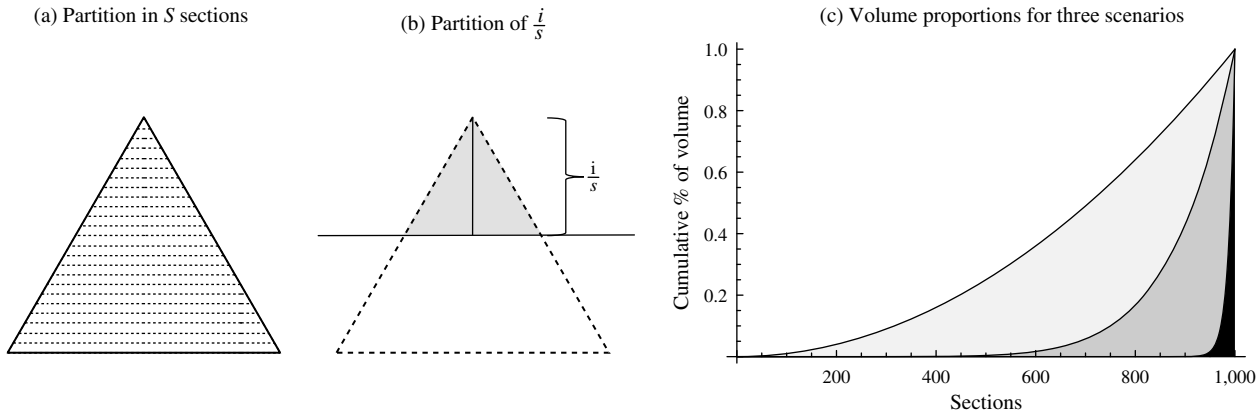

Note. Where scenarios for one, two, and four random variables are shaded light gray, dark gray, and black, respectively.

is larger, the total n-content $\sqrt{n+1}/n!$ decreases to zero as n goes to infinity. This decay occurs more quickly in the corners of the polytope.

References

Abbas AE (2006) Entropy methods for joint distributions in decision analysis. *IEEE Trans. Engrg. Management* 53(1):146–159.

Apostolakis G, Kaplan S (1981) Pitfalls in risk calculations. *Reliability Engrg.* 2(2):135–145.

Ben-Tal A, Ghaoui LE, Nemirovski A (2009) *Robust Optimization* (Princeton University Press, Princeton, NJ).

Bickel JE, Smith JE (2006) Optimal sequential exploration: A binary learning model. *Decision Anal.* 3(1):16–32.

Bickel JE, Lake LW, Lehman J (2011) Discretization, simulation, and Swanson's (inaccurate) mean. *SPE Econom. Management* 3(3):128–140.

Bickel JE, Smith JE, Meyer JL (2008) Modeling dependence among geologic risks in sequential exploration decisions. *Reservoir Eval. Engrg.* 3(4):233–251.

Chessa AG, Dekker R, Van Vliet B, Steyerberg EW, Habbema JDF (1999) Correlations in uncertainty analysis for medical decision making: An application to heart-valve replacement. *Medical Decision Making* 19(3):276–286.

Clemen RT (1996) *Making Hard Decisions. An Introduction to Decision Analysis*, 2nd ed. (Duxbury Press, Belmont, CA).

Clemen RT, Reilly T (1999) Correlations and copulas for decision and risk analysis. *Management Sci.* 45(2):208–224.

Cooke RM, Waij R (1986) Monte Carlo sampling for generalized knowledge dependence with application to human reliability. *Risk Anal.* 6(3):335–343.

Frees EW, Carriere J, Valdez EA (1996) Annuity valuation with dependent mortality. *J. Risk Insurance* 63(2):229–261.

Ireland CT, Kullback S (1968) Contingency tables with given marginals. *Biometrika* 55(1):179–188.

Jaynes ET (1957) Information theory and statistical mechanics. *Physical Rev.* 106(4):620–630.

Jaynes ET (1968) Prior probabilities. *IEEE Trans. Systems Sci. Cybernetics* 4(3):227–241.

Jimenez L, Landgrebe D (1998) Supervised classification in high dimensional space: Geometrical, statistical and asymptotical properties of multivariate data. *IEEE Trans. Systems, Man, Cybernetics* 28(1):39–54.

Jouini MN, Clemen RT (1996) Copula models for aggregating expert opinions. *Oper. Res.* 44(3):444–457.

Keefer DL, Bodily SE (1983) Three-point approximations for continuous random variables. *Management Sci.* 29(5):595–609.

Korsan RJ (1990) Towards better assessment and sensitivity procedures. Oliver RM, Smith JQ, eds. *Influence Diagrams, Belief Nets and Decision Analysis* (John Wiley & Sons, New York), 427–454.

Lowell DG (1994) Sensitivity to relevance in decision analysis. Ph.D. thesis, Engineering and Economic Systems, Stanford University, Stanford, CA.

MacKenzie GR (1994) Approximately maximum entropy multivariate distributions with specified marginals and pairwise correlations. Ph.D. thesis, Department of Decision Sciences, University of Oregon, Eugene.

Miller AC (1990) Towards better assessment and sensitivity procedures by R. J. Korsan: Discussion by Allen C. Miller. Oliver RM, Smith JQ, eds. *Influence Diagrams, Belief Nets and Decision Analysis* (John Wiley & Sons, New York), 442–443.

Montiel LV (2012) Approximations, simulation, and accuracy of multivariate discrete probability distributions in decision analysis. Ph.D. thesis, University of Texas at Austin, Austin.

Montiel LV, Bickel JE (2012) Generating a random collection of discrete joint probability distributions subject to partial information. *Methodology Comput. Appl. Probab.*, ePub ahead of print May 22, http://www.springerlink.com/content/263823150021hl36/.

Nelsen RB (1991) Copulas and association. Dall'Aglio G, Kotz S, Salinetti G, eds. *Advances in Probability Distributions with Given Marginals* (Kluwer Academic, Dordrecht, The Netherlands), 51–74.

Nelsen RB (2005) *An Introduction to Copulas*, 2nd ed. (Springer, Portland, OR).

Nešlehová J (2007) On rank correlation measures for non-continuous random variables. *J. Multivariate Anal.* 98(3):544–567.

Pearson ES, Tukey JW (1965) Approximate means and standard deviations based on distances between percentage points of frequency curves. *Biometrika* 52(3/4):553–546.

Presidential Commission on the Space Shuttle Challenger Accident (1986) Report of the Presidential Commission on the Space Shuttle Challenger Accident. Presidential Commission on the Space Shuttle Challenger Accident, Washington, DC.

Reilly T (2000) Sensitivity analysis for dependent variables. *Decision Sci.* 31(3):551–572.

Sklar A (1959) Fonctions de répartition à n dimensions et leurs marges. *Publ. Inst. Statist. Univ. Paris* 8:229–231.

Smith JE (1993) Moment methods for decision analysis. *Management Sci.* 39(3):340–358.

Smith RL (1984) Efficient Monte Carlo procedures for generating points uniformly distributed over bounded regions. *Oper. Res.* 32(6):1296–1308.

Smith RL, Ryan PB, Evans JS (1992) The effect of neglecting correlations when propagating uncertainty and estimating the population distribution of risk. *Risk Anal.* 12(4):467–474.

Wang T, Dyer JS (2012) A copulas-based approach to modeling dependence in decision trees. *Oper. Res.* 60(1):225–242.

Winkler RL (1982) Research directions in decision making under uncertainty. *Decision Sci.* 13(4):517–533.